Power Efficient Modulation Scheme CDM^2-MAP for Low Complexity and High Performance

Ho Van Khuong, Hyung Yun Kong, and Doo Hee Nam

Abstract: **Quadrature amplitude modulation-spread spectrum (QAM-SS) and code division multiplexing (CDM) are multi-level modulation schemes with high performance but they cause a large peak-average power ratio (PAPR). Therefore, this paper proposes a novel modulation scheme for high-rate transmission which follows a sequence of CDM-mapping-CDM not only to correct the above-mentioned problem but also offer a high flexibility in obtaining arbitrary multilevel modulation with very low implementation complexity and high performance.**

Index Terms: **Code division multiplexing (CDM), mapping, peak-average power ratio (PAPR), quadrature amplitude modulation (QAM).**

I. INTRODUCTION

The next generation communication systems are expected to meet a drastically increasing demand of information, communication, and entertainment services such as voice, data, image, video, etc, which can be accessed anywhere at anytime. There are multiple solutions to achieve this aim and one of them is the devise of the advanced modulation and demodulation techniques. Mc (multi-code)-modulation has been proposed for supporting high data rates as well as multi-media wireless communications in W-CDMA system but it has a serious problem of large amplitude fluctuation because the amplitude levels constructed by successive "zeros" or "maximum value" sequences often appear [1]–[2]. An alternative high-efficiency modulation technique is QAM which can achieve both higher data-rate and variable rate. However, the main disadvantage of such modulation is its sensitivity to nonlinear amplifiers, recovery of carrier, high PAPR, etc. Moreover, a combination of Mc-modulation and QAM was also suggested to yield a high-rate transmission for 2.4 GHz-band wireless LAN system [3] but it exhibits high PAPR values and a significant performance (in terms of BER) degradation. Recently, the complex spreading sequences which expose an interesting feature of low PAPR have found some applications in W-CDMA yet still suffer a high error probability in multi-path fading channels [4].

In order to correct the deficiency of the above modulation schemes, we propose a single-user multi-level modulation technique, in the sequel referred to as CDM^2-MAP, whose operation mechanism is as follows. The input data-stream is organized into blocks, each of which is code-division multiplexed first. Then the resulting outputs are mapped into the M-PSK signal constellations with different phase-offsets and finally, they are spectrum-spread again by a CDM set. By doing so, we will prove that the suggested technique can achieve simultaneously many targets such as high performance, low PAPR, high data rate, and low implementation complexity.

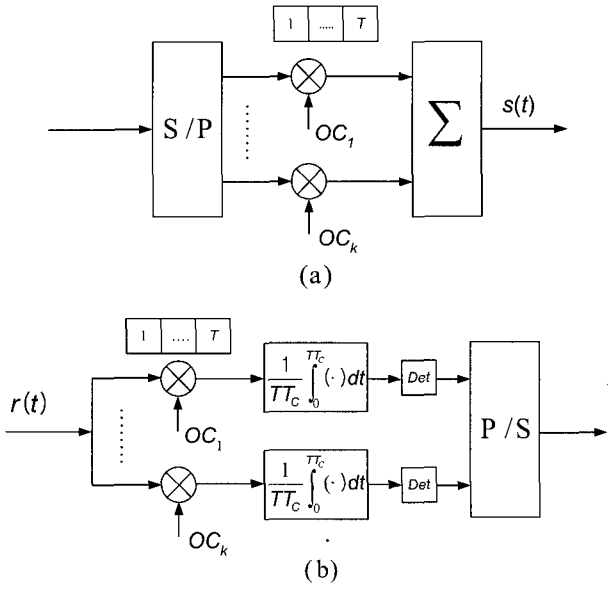

Fig. 1. Multi-code modem: (a) Modulator and (b) demodulator.

The rest of the paper is organized as follows. Section II summarizes the conventional Mc-modulation to point out its disadvantages. Then, all details on the proposed modulation technique are introduced in Section III and simulation results are presented in Section IV. Finally, the paper ends with conclusion in Section V.

II. CONVENTIONAL MULTI-CODE MODULATION

Fig. 1 illustrates the block diagram of Mc-modem. The high-speed data stream is serial-to-parallel converted into K lower-rate sub-streams, each of which is spread by orthogonal codes (OCs) of length T which are usually Walsh-Hadamard ones. The resulting signals are summed together to generate the following waveform

$$s(t) = \sum_{k=1}^{K} a_k \sum_{i=1}^{T} OC_k(i) p(t - iT_c) \tag{1}$$

where a_k is the modulated data-symbol of k-th branch with time duration KT_s (T_s denotes input data-symbol period); $OC_k(i)$ represents the i-th chip of the k-th OC; $p(t)$ is a unit amplitude rectangular pulse with T_c-width; T_c denotes chip duration. In

Manuscript received January 11, 2005; approved for publication by Marco Lops, Division I Editor, August 29, 2005.

The authors are with the Department of Electrical Engineering, University of Ulsan, Korea, email: khuongho2001@yahoo.com, {hkong, duheeya}@mail.ulsan.ac.kr.

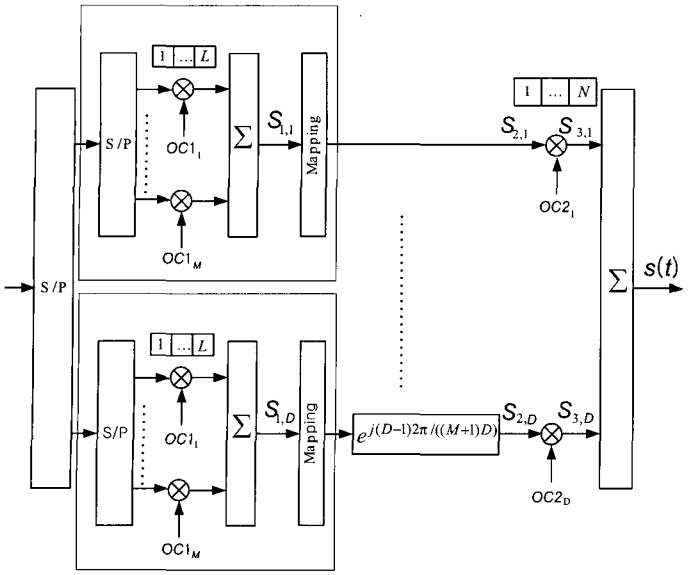

Fig. 2. Block diagram of CDM^2-MAP modulator.

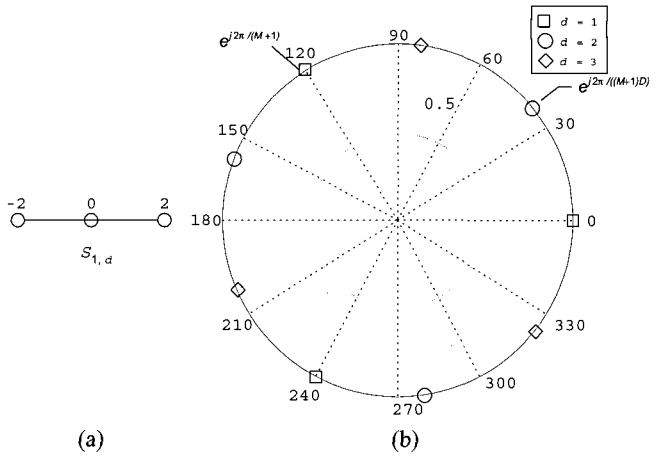

Fig. 3. Mapping technique $M = 2, D = 3$: (a) Possible output values of the 1st CDM and (b) mapping technique for each substream.

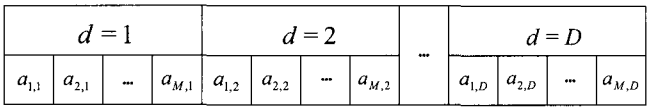

Fig. 4. Structure of D data groups.

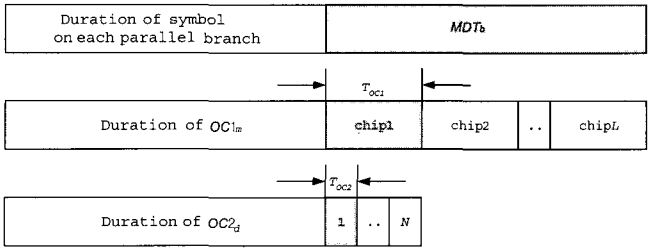

Fig. 5. Time periods of some signals.

this paper, if a_k is BPSK-modulated, the modulation technique is called C-CDM (conventional CDM) [5] and if a_k is QAM-modulated then it is called QAM-SS [3] in which only gray-coded square constellations are considered.

A linear combination of OCs can create successive "zero" sequences or "maximum value" sequences, and thus causing a large amplitude variation which reduces the efficiency of nonlinear amplifiers. For C-CDM, the peak power of signal $s(t)$ can be up to K^2 and $2(KQ)^2$ for QAM-SS where Q is maximum value of real part of complex QAM-symbol a_k. In addition, in order to increase bit-rate and BER performance, long OCs are needed which bring about difficulty in hardware implementation.

III. PROPOSED MODULATION SCHEME

The structure of suggested CDM^2-MAP modulator is shown in Fig. 2. The BPSK-modulated data stream of MD symbols with bit-rate $R_b = 1/T_b$ is split into D lower-rate parallel streams. Then each substream is modulated by C-CDM technique. The output signals after the 1st CDM are given by

$$S_{1,d}(i) = \sum_{m=1}^{M} a_{m,d} OC1_m(i) \tag{2}$$

where $OC1_m(i)$ is the i-th chip of m-th orthogonal spreading code of length L and time duration T_{OC1} which is chosen as Walsh-Hadamard code; $a_{m,d}$ represents m-th data-symbol on d-th large branch; $d = 1, \cdots, D$.

Sequentially, the symbols $S_{1,d}(i)$ are mapped to $(M+1)$-PSK constellations and phase-shifted from each other by an amount of $(d-1)2\pi/((M+1)D)$ to avoid the in-phase combination which causes high PAPR before code-division multiplexed once again (see Fig. 3). Finally, the resulting signals are added together to produce a signal as

$$s(t) = \sum_{d=1}^{D} S_{2,d}(i) \sum_{n=1}^{N} OC2_d(n) g(t - nT_{OC2}). \tag{3}$$

Here

$$S_{2,d}(i) = e^{j\pi S_{1,d}(i)/(M+1)} e^{j(d-1)2\pi/((M+1)D)} \tag{4}$$

and $OC2_d(n)$ is the n-th chip of length-N Walsh-Hadamard code with chip duration T_{OC2}; $g(t)$ is a unit-amplitude rectangular pulse with width T_{OC2}.

In aspect of hardware implementation, it is obvious that this is a very simple modulator consisting of identical D CDM-mapping sets operated in parallel, a phase-shift block and CDM. Moreover, variable high speed-data transmission is easily obtained by changing the combination (D, M, L, N) without increasing the implementation complexity due to the usage of the short OCs ($OC1$ and $OC2$).

For the proposed modulation technique, there are two spread-spectrum operations with different processing gains L and N but their functions are distinct: $OC2_d$ to distinguish each branch and the other $OC1_m$ to discriminate the data symbols within the same branch. Based on Figs. 4 and 5, some relationships are established as follows

$$M \leq L \tag{5}$$

$$\frac{R_b}{R_{OC2}} = \frac{T_{OC2}}{T_b} = \frac{MD}{LN} \tag{6}$$

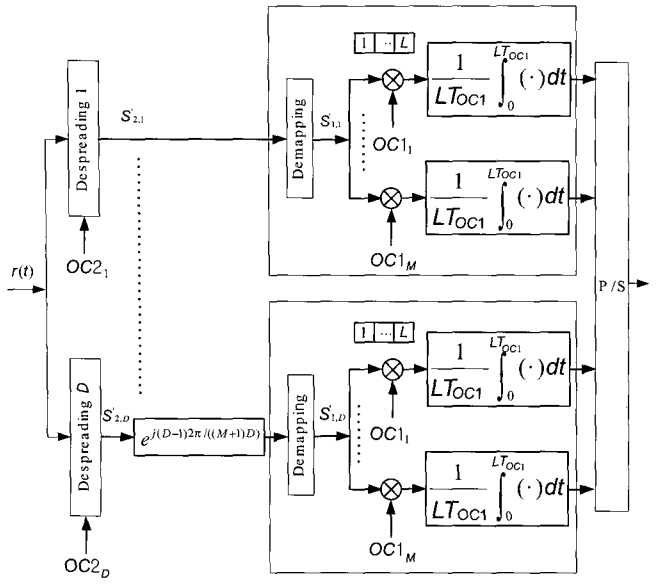

Fig. 6. Block diagram of the proposed base-band demodulator.

Table 1. Simulation parameters for Figs. 7–10 and theoretically calculated-PAPR for three modulation schemes.

QAM-SS (PG= 64)			
Levels	$T_b/T_c = T/(KY)$		PAPR
256	64/8		2.6471
64	64/6		2.3333
16	64/4		1.8000
C-CDM			
Levels	$T_b/T_c = T/K$	(K,T)	PAPR
256	64/8	(1,8)	1
64	64/6		1
16	64/4	(1,16)	1
Proposed ($M \leq L$)			
Levels	$T_b/T_{OC2} = NL/(MD)$	(D, M, L, N)	PAPR
256	64/8	(1, 2, 2, 8)	1
64	64/6	(1, 3, 4, 8)	1
16	64/4	(1, 2, 2, 16)	1

where R_{OC2} is the chip-rate of $OC2_d$.

The ratio $\eta_P = R_b/R_{OC2}$ is defined as bandwidth efficiency. Similarly, bandwidth efficiency of C-CDM and 2^Y-QAM-SS can be calculated (see Fig. 1) as $\eta_{C-CDM} = R_b/R_{OC} = K/T$ and $\eta_{QAM-SS} = R_b/R_{OC} = KY/T$, respectively.

The maximum transmitted power of the proposed modulator only occurs when output signals of all branches $S_{2,d}$ fall in the same arc $[0, 2\pi(D-1)/((M+1)D)]$. This peak power is denoted as $P_{peak,P}$ which can be computed based on Fig. 3 as

$$P_{peak,P} = \left| \sum_{g=0}^{D-1} e^{jg2\pi/((M+1)D)} \right|^2 = \left(\frac{\sin[\frac{\pi}{(M+1)}]}{\sin[\frac{\pi}{((M+1)D)}]} \right)^2. \tag{7}$$

The demodulation process is in the inverse order of modulation as shown in Fig. 6. First, the mapped symbols are roughly estimated by despreading the received signal $r(t)$ to generate $S'_{2,d}(k)$. These despreaders are very diversified such as multi-user detectors [5], rake demodulators [6] for multi-path fading channels or simply chip matched-filters for additive white Gaussian noise (AWGN) channels. For example in AWGN channels, $S'_{2,d}(k)$ can be detected by correlating $r(t)$ with the replicas of $OC2_d$

$$S'_{2,d}(k) = \frac{1}{NT_{OC2}} \int_0^{NT_{OC2}} r(t) OC2_d(n) g(t - nT_{OC2}) dt. \tag{8}$$

The resultant signals are phase-shifted by an amount $-(d-1)2\pi/((M+1)D)$ corresponding to its branch number to compensate for the phase-offset added at the modulator. Afterward, de-mapping to regenerate PAM signal is performed by first finding $S_2(i)$ among all available $(M+1)$-PSK signal constellations so that the Euclidean distance between $S'_{2,d}(k)$ and $S_2(i)$ is smallest

$$\min_{all\ S_2(i)} |S'_{2,d}(k) - S_2(i)|^2. \tag{9}$$

Then looking-up the position of $(M+1)$-PSK constellation point $S_2(i)$ in the mapping table will yield the corresponding PAM signals $S'_{1,d}$.

Ultimately, the detection of original data symbols is performed by de-spreading $S'_{1,d}$ with $OC1_m$

$$a'_{m,d} = sgn\left(\frac{\int_0^{LT_{OC1}} S'_{1,d}(t) OC1_m(n) g(t - nT_{OC1}) dt}{LT_{OC1}} \right) \tag{10}$$

where $a'_{m,d}$ represents the detected symbol of the original symbol $a_{m,d}$ and $sgn(\cdot)$ denotes the signum function.

Once again, it is found that the demodulator can be implemented in a very simple way because the same CDM blocks are reused in parallel to decode the data.

IV. SIMULATION RESULTS

In this part, we evaluate the BER performance of the proposed modulation technique in pure AWGN channel and multi-path Rayleigh fading channel plus AWGN.

A. AWGN Channel

The BER performance and PAPR of three modulation techniques: QAM-SS [3], C-CDM [5], and CDM^2-MAP in AWGN environment are compared together under the same conditions of the bit-rate and transmission bandwidth; that means the ratio T_b/T_{OC} is the same for all techniques. These criteria require the appropriate parameters for each modulation format which are listed in Table 1 where the reference scheme is 2^Y-QAM-SS with constant processing gain of 64 (PG= 64). Also, the smallest PAPR of each scheme which is acquired as the number of parallel branches equals 1 is presented in this table. It is realized that C-CDM and CDM^2-MAP exhibit a constant PAPR while PAPR of QAM-SS is very high and fluctuates over a large range as the number of modulation levels increases.

Investigation of PAPR and BER is demonstrated in Figs. 7–10 when the number of branches changes; that is, D and K are

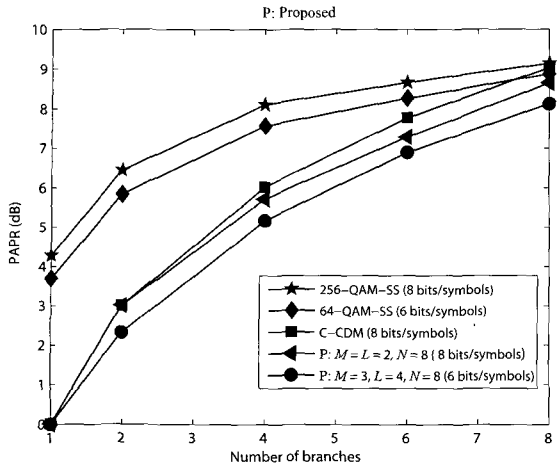

Fig. 7. PAPR comparison for cases of 8 bits/symbol and 6 bits/symbol.

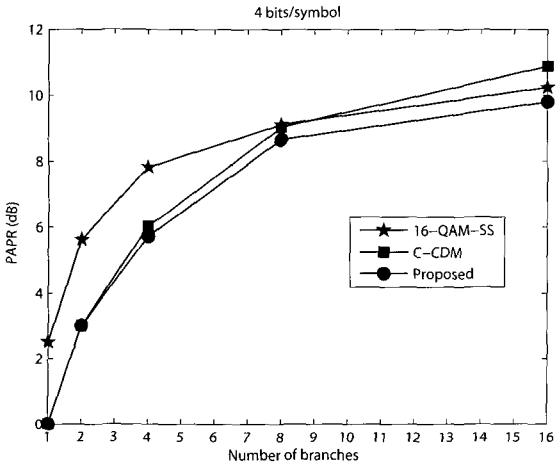

Fig. 8. PAPR comparison for case of 4 bits/symbol.

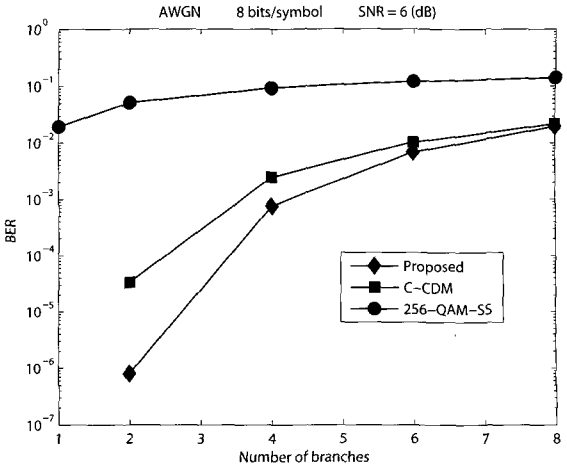

Fig. 9. PBER comparison among CDM^2-MAP, 256-QAM-SS, and C-CDM.

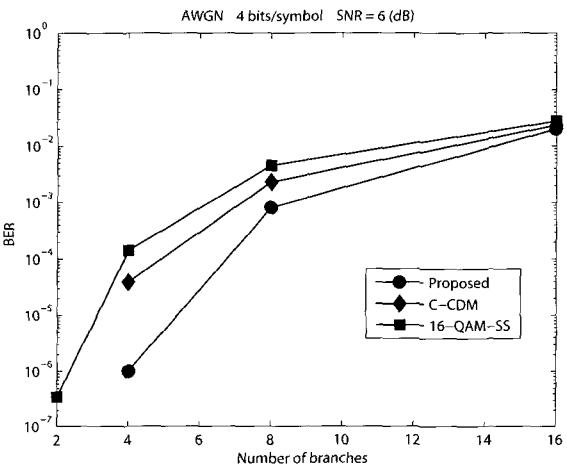

Fig. 10. BER comparison among CDM^2-MAP, 16-QAM-SS, and C-CDM.

varied but the other simulation parameters are similar to those given in Table 1 to keep all modulation schemes have similar bit-rate and chip-rate.

In Figs. 7 and 8, 10000 data symbols are used for computing average PAPR for each modulation scheme. It is seen that PAPR of the proposed scheme is extremely low compared to those of C-CDM and QAM-SS. This is logical because it prevents the signals of branches from in-phase summation as well as destructive superposition owing to the phase-offset introduced among branches.

A superiority of the proposed scheme in achieving a better performance than the others as the data-rate increases is illustrated in Figs. 9 and 10. We find that the more the number of modulation levels increases, the larger performance improvement.

The proposed modulation technique benefits from the flexibility in obtaining the arbitrarily high number of modulation levels by simply choosing a combination (D, M, L, N) for satisfying (6). This is verified through a list of parameters for use in simulation for CDM^2-MAP given in Table 2 where we expect to achieve the same number of modulation levels as the reference

Table 2. Simulation parameters for different modulation level number of the proposed technique.

QAM-SS (PG= 64, $K = 1$)	Proposed technique ($M \leq L$)	
Levels	$T_b/T_{OC2} = NL/(MD)$	(D, M, L, N)
16	64/4	(1, 2, 2, 16)
32	64/5	(1, 5, 8, 8), (5, 2, 2, 64)
64	64/6	(1, 3, 4, 8), (3, 2, 2, 32)
128	64/7	(1, 7, 8, 8), (7, 2, 2, 64)
256	64/8	(1, 2, 2, 8)
512	64/9	(1, 9, 16, 4), (3, 3, 4, 16), (9, 2, 2, 64)
1024	64/10	(1, 5, 8, 4), (5, 2, 2, 32)

scheme 2^Y-QAM-SS with PG= 64. It is found that there are multiple choices to design a multilevel modulator; for example, a modem of 512 levels can be generated from three sets (D, M, L, N) : $(1, 9, 16, 4), (3, 3, 4, 16), (9, 2, 2, 64)$. More-

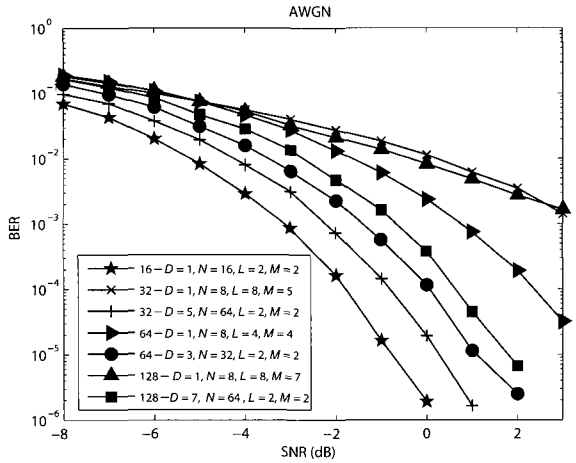

Fig. 11. BER of CDM^2-MAP for modulation levels 16, 32, 64, 128.

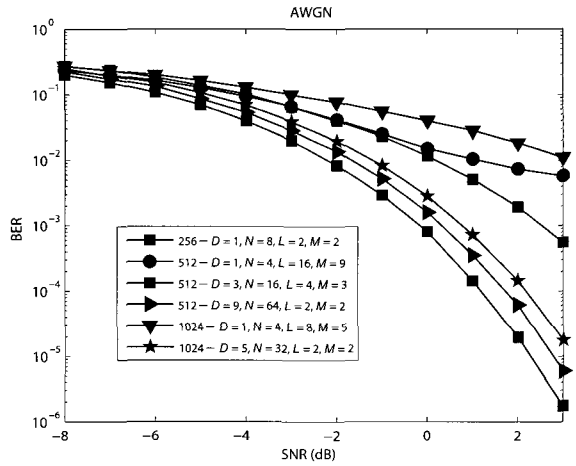

Fig. 12. BER of CDM^2-MAP for modulation levels 256, 512, and 1024.

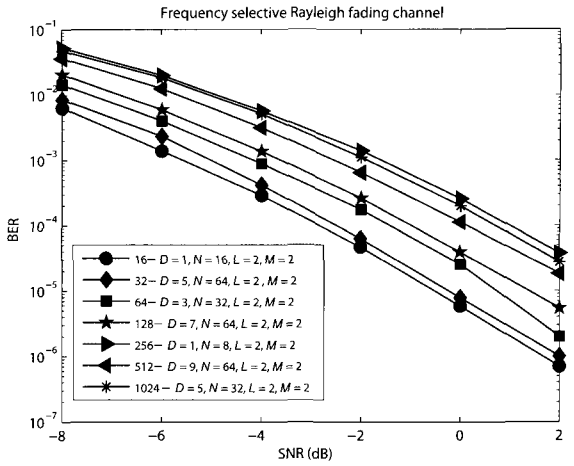

Fig. 13. BER of CDM^2-MAP for different modulation levels equivalent to QAM-SS of 16, 32, 64, 128, 256, 512, and 1024 levels in multi-path Rayleigh fading channel.

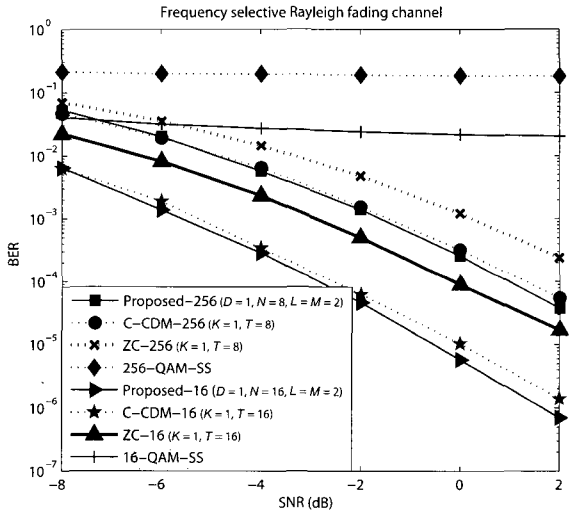

Fig. 14. BER comparison among CDM^2-MAP, QAM-SS, C-CDM, and spread spectrum with Zadoff Chu sequences in multi-path Rayleigh fading channel.

over, the formula (6) also exposes that the optimum bandwidth efficiency can only be achievable with $L = M$.

Figs. 11 and 12 plot the BER performance of the multi-level modulator constructed by the proposed scheme. Because there are two spread-spectrum operations but the second one is more important than the first since it helps distinguish data groups of each branch before detecting data symbols separately, among selections (D, M, L, N) fulfilling (6) we should choose $L = M$ as small as possible to obtain an optimum bandwidth efficiency and reduce the constellation size and N as large as possible to increase the processing gain for the data branches. These simulations strongly support the above comments in obtaining high performance for any modulation level. The cases of $L = M = 2$ and large N always offer better performance than the asymmetrical cases $L \neq M$.

B. Frequency Selective Rayleigh Fading Channel

A frequency selective Rayleigh fading channel under investigation has a slow fading rate compared to the symbol rate so that the channel random parameters do not change significantly over several symbol intervals. For such a channel, it can be modeled as the tapped delay line (TDL) channel model [6] with the complex low-pass equivalent impulse response given by

$$h(t) = \sum_{l=1}^{L} \alpha_l e^{j\theta_l} \delta(t - \tau_l) \tag{11}$$

where $\alpha_l, \theta_l, \tau_l$, and L are the gain, the phase, the delay of the l-th path and the number of paths, correspondingly, and $\delta(\cdot)$ is the Dirac delta function. In this paper, the number of paths is limited to $L = 5$ with $\tau_l = lT_{OC2}$ and time-varying tap weights $\alpha_l e^{j\theta_l}$ are assumed to be equal-power mutually uncorrelated random variables of which the magnitudes are Rayleigh-distributed and the phases are uniformly distributed over $[0, 2\pi]$. Moreover, for simplicity, the power of each path is chosen to equal 1.

Fig. 13 illustrates the BER performance of the proposed mod-

ulation technique for distinct modulation levels corresponding to the different combinations of (D, M, L, N) given in Table 2 in frequency-selective Rayleigh fading channel plus AWGN using rake demodulator with 5 fingers and a maximum ratio combining technique [6] for all despreading blocks (see Fig. 6) under assumption that the path delay and the channel state are perfectly estimated. It is realized that although its performance is degraded by fading environment in comparison to that in case of AWGN, this performance is still practically acceptable in such a harsh channel.

The simulation result in Fig. 14 illustrates the difference in the BER performance between the existing modulation schemes and the proposed one under the identical bit-rate and transmission bandwidth. We keep the same simulation conditions including the propagation environment, detector and channel state information as for Fig. 13. The integers following the modulation technique in the legend box represent the number of modulation levels which is equivalently considered to that of QAM-SS; for example, proposed-256 means the proposed technique that can yield 256 levels as 256-QAM-SS. It is well-known that the spread spectrum modulation gains the best performance when the number of spreading codes equals 1 and rake's receiver with MRC is used. Therefore, we consider this optimum case to compare the performances of the modulation techniques in terms of the modulation level number and BER. As seen in Fig. 14, QAM-SS's performance degrades severely in fading channels and is the worst among three examined competing techniques since it is very sensitive to the changes in the phase and amplitude of the carrier. Moreover, it is recognized that the CDM^2-MAP method shows a slight performance improvement relative to C-CDM for any modulation level at low SNR but when the SNR increases, the CDM^2-MAP considerably outperforms C-CDM due to its steeper BER curves than those of C-CDM; specifically, at BER of 10^{-6}, the proposed technique yields a gain of about 1dB compared to C-CDM with 16 modulation levels.

Simulation parameters in Fig. 14 result in the PAPR of 1 for both C-CDM and CDM^2-MAP. This figure also depicts the BER graphs of spread spectrum technique with PAPR of 1 and BPSK data-modulation using Zadoff Chu (ZC) sequences with lengths of 8 and 16. Their performance with different lengths is denoted as ZC-16 and ZC-256, correspondingly which are considered as 16 and 256-level modulators under the identical bit-rate and transmission bandwidth as for 16-QAM-SS and 256-QAM-SS. Fig. 14 shows that ZC sequences suffer the performance degradation in multipath fading channels and are significantly worse than C-CDM and CDM^2-MAP.

V. CONCLUSION

A new modulation scheme CDM^2-MAP is proposed in this paper. With a special mapping technique, this modulator guarantees a lower PAPR than those of QAM-SS and C-CDM. Moreover, the combination (D, N, L, M) makes the modulator flexible in altering modulation levels (or variable high data rate) as well as easily implementing in hardware as a direct consequence of applying short orthogonal codes. The simulation results in AWGN and multi-path Rayleigh fading channel revealed its high robustness against the adverse effects of propagation environment. Thus, it should be considered as a prominent candidate for high data speed future communications systems.

ACKNOWLEDGMENTS

The authors would like to thank the editor and the anonymous reviewers for their helpful comments and suggestions in improving the original manuscript.

This work was supported by grant No. (R05-2004-000-11066-0) from Ministry of Science & Technology.

REFERENCES

[1] N. Guo and L. B. Milstein, "On sequence sharing for multi-code DS/CDMA systems," in *Proc. MILCOM'98*, (Boston, USA), vol. 1, Oct. 1998, pp. 238–242.

[2] N. Iwakiri, "Evaluation of multilayer high-speed data transmission based on multi-code technology," in *Proc. ICT'98*, (Porto Carras, Greece), vol. 1, June 1998, pp. 489–493.

[3] K. Watanabe, S. Miyamoto, and N. Morigana, "Adaptive multi-code transmission with adaptive multilevel modulation for 2.4 GHz-band wireless LAN systems," *Proc. IEEE*, vol. 39, no. 1, pp. 168–170, Jan. 2003.

[4] L. Staphorst, M. Jamil, and L. P. Linde, "Performance evaluation of a QPSK system employing complex spreading sequences in a fading environment," in *Proc. VTC'99-Fall*, vol. 5, Sept. 1999, pp. 2964–2968.

[5] S. L. Miller and W. Tantiphaiboontana, "Code division multiplexing-efficient modulation for high data rate transmission over wireless channels," in *Proc. IEEE ICC 2000*, vol. 3, June 2000, pp. 1487–1491.

[6] J. G. Proakis, *Digital Communications*, 4-th ed., McGraw-Hill, 2001.

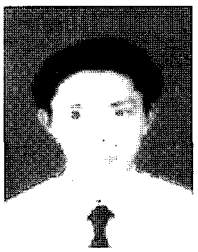

Ho Van Khuong received the B.E. and the M.S. degrees in Electronics and Telecommunications Engineering from HoChiMinh City University of Technology, Vietnam, in 2001 and 2003, respectively. From April 2001 to September 2004, he was a lecturer at Telecommunications Department, HoChiMinh City University of Technology. He is currently working toward the Ph.D. degree in the Department of Electrical Engineering, University of Ulsan, Korea. His major research interests are modulation and coding techniques, MIMO system, digital signal processing, and cooperative communications.

Hyung Yun Kong received the Ph.D. and M.E. degrees in Electrical Engineering from Polytechnic University, Brooklyn, New York, USA, in 1996 and 1991, respectively. And he received B.E. in Electrical Engineering from New York Institute of Technology, New York in 1989. Since 1996, he was with LG electronics Co., Ltd. in multimedia research lab. developing PCS mobile phone systems and LG chair man's office planning future satellite communication systems from 1997. Currently, he is an associate professor in Electrical Engineering at University of Ulsan, Ulsan, Korea. He performs several government projects supported by ITRC (Information Technology Research Center), KOSEF (Korean Science and Engineering Foundation), etc. His research area includes high data rate modulation, channel coding, detection and estimation, cooperative communications, and sensor network. He is a member of IEEK, KICS, KIPS, and IEICE.

Doo Hee Nam received the B.E. degree in Electrical Engineering from University of Ulsan, Ulsan, Korea in 2004. Currently, he is a master degree candidate in Electrical Engineering at the same university from 2004. And he is pursuing M.E. degree under the advice of Prof. Hyung Yun Kong. He also participates a project supported by KOSEF (Korean Science and Engineering Foundation) and ITRC (Information Technology Research Center). His research area includes multi-code modulation, LDPC, and sensor network.